

# Ultrafast polarization and magnetization response of multiferroic GaFeO<sub>3</sub> using time-resolved nonlinear optical techniques

Masakazu Matsubara,<sup>1,2</sup> Yoshio Kaneko,<sup>3</sup> Jin-Ping He,<sup>3</sup> Hiroshi Okamoto,<sup>1,2,4</sup> and Yoshinori Tokura<sup>1,3,5</sup>

<sup>1</sup>National Institute of Advanced Industrial Science and Technology (AIST), Tsukuba 305-8562, Japan

<sup>2</sup>CREST, Japan Science and Technology Agency (JST), Kawaguchi, Saitama 332-0012, Japan

<sup>3</sup>Multiferroics Project, ERATO, Japan Science and Technology Agency (JST), ASI, RIKEN, Wako 351-0198, Japan

<sup>4</sup>Department of Advanced Materials Science, University of Tokyo, Chiba 277-8561, Japan

<sup>5</sup>Department of Applied Physics, University of Tokyo, Tokyo 113-8656, Japan

(Received 20 February 2009; published 29 April 2009)

We have investigated the ultrafast electric and magnetic response of multiferroic GaFeO<sub>3</sub> induced by irradiation of a femtosecond laser pulse. By using the polarization selection rules of crystallographic and magnetic second-harmonic generation, the dynamics of electric polarization  $P$  and toroidal moment  $T$  were simultaneously and separately detected on a femtosecond time scale. The magnetization dynamics was derived by comparing the dynamics of  $P$  and  $T$ . We demonstrate the availability of time-resolved nonlinear optical techniques for the dynamical probe of multiple degrees of freedom in multiferroics.

DOI: 10.1103/PhysRevB.79.140411

PACS number(s): 75.50.Gg, 77.22.Ej, 78.47.J-, 42.65.Ky

Materials with several coexisting order parameters relevant to electricity and magnetism is referred to as multiferroics. On the basis of cross correlation between the ferroelectric polarization and ferromagnetic magnetization, it may be possible to control the magnetization by electric fields and/or the polarization by magnetic fields. The recent discovery of the strong coupling between ferroelectricity and magnetism in a multiferroic material<sup>1</sup> has triggered the revival of the studies of such magnetoelectric (ME) effects.<sup>2,3</sup> When we consider the application of multiferroic systems to future electronics and/or spintronics, it is essentially important to clarify dynamical properties of charges (or polarization) and spins (or magnetization). In spite of the rapidly increasing interest in the multiferroic systems, their dynamical aspects have hardly been studied as yet.

In the present study, we have investigated the ultrafast electric polarization  $P$  and magnetization  $M$  dynamics in GaFeO<sub>3</sub>, a representative of multiferroic materials. GaFeO<sub>3</sub> is a pyroelectric ferrimagnet, in which spontaneous  $P$  and  $M$  coexist at low temperatures. Figure 1(a) shows the crystal structure of GaFeO<sub>3</sub>. In an orthorhombic unit cell, there are two crystallographically unequivalent Fe sites referred to as Fe1 and Fe2 and Ga sites as Ga1 and Ga2. The Fe1 and the Fe2 sites are shifted by +0.26 Å and -0.11 Å from the center positions of the FeO<sub>6</sub> octahedra, respectively. Due to these fairly large displacements,  $P$  appears along the  $b$  axis. In addition, below the ferrimagnetic transition temperature ( $T_C \sim 205$  K), the spin moments of the Fe1 and the Fe2 sites are parallel and antiparallel to the  $c$  axis, respectively. Since some portion of the Ga ions occupy the Fe sites due to the similar ion sizes, the occupations of the Fe ions in the Fe1 and the Fe2 sites are different from each other. As a result, GaFeO<sub>3</sub> shows a ferrimagnetic property with the easy axis along the  $c$  direction. Moreover, GaFeO<sub>3</sub> possesses a toroidal moment  $T$  along the  $a$  axis. Here, the toroidal moment is described by  $T \propto \sum_i r_i \times s_i$ ,  $r_i$  and  $s_i$  being the electron coordination and spin moment at the magnetic (Fe) site  $i$ .<sup>4-7</sup> In GaFeO<sub>3</sub>, the local  $r_i \times s_i$  show ferroic alignments along the  $a$  axis, as shown in Fig. 1(a). Such a ferrotoroidic nature in

GaFeO<sub>3</sub> has led to the successful observation of correlation effects between magnetism and dielectricity; the ME effect,<sup>4,5</sup> its optical frequency version (optical ME effect) in near infrared to visible region<sup>8</sup> and x-ray region<sup>9,10</sup> and also the magnetization-induced second-harmonic (SH) generation (SHG) (MSHG).<sup>11,12</sup> These studies suggest that GaFeO<sub>3</sub> is a suitable material for the investigation of dynamical aspects of the electric/magnetic response and their interaction.

To probe the dynamical behaviors of multiferroic properties, we have utilized the MSHG. Up until now, MSHG has been used as a valuable tool for the investigation of the magnetic properties, especially of thin films and multilayers, due to its intrinsic surface and interface sensitivity.<sup>13</sup> It has also been shown that MSHG can be a powerful tool for the investigation of the noncentrosymmetric-antiferromagnetic or multiferroic materials.<sup>6,14,15</sup> Therefore, we can consider that

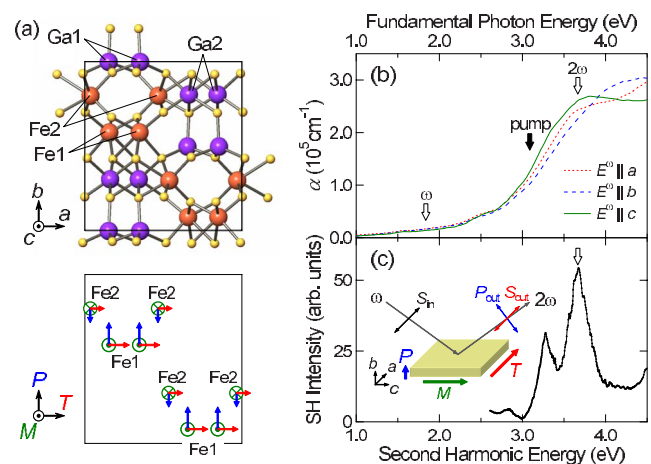


FIG. 1. (Color online) (a) Crystal structure of a multiferroic GaFeO<sub>3</sub>. The electric polarization  $P$ , the magnetization  $M$ , and the toroidal moment  $T$  are generated along the  $b$ ,  $c$ , and  $a$  axes, respectively. (b) Absorption spectra of GaFeO<sub>3</sub> (see text). (c) MSHG spectrum in the  $S_{in}$ - $S_{out}$  configuration at 10 K, which is cited from Ref. 11. Inset shows the schematic of the experimental configuration for SHG and MSHG.

time-resolved MSHG is a promising approach for the detection of the ultrafast dynamics in multiferroic systems.

The expression for the second-order nonlinear polarization  $P_i(2\omega)$  in the presence of magnetization can be written in the form,

$$P_i(2\omega) = \sum_{j,k} \epsilon_0 (\chi_{ijk}^c + \chi_{ijk}^m) E_j(\omega) E_k(\omega), \quad (1)$$

where  $\chi^c$  and  $\chi^m$  are the second-order nonlinear susceptibilities  $\chi^{(2)}$  related to the crystallographic SHG and MSHG, respectively. The magnetic space group of GaFeO<sub>3</sub> is  $Pc2_1n$  in the ferrimagnetic phase with the spontaneous  $M$  along the  $c$  axis. Upon the irradiation of  $s$ -polarized ( $E^\omega \parallel a$ ) fundamental light on the  $ac$  surface of GaFeO<sub>3</sub> [the inset of Fig. 1(c)], the nonzero components of  $\chi^{(2)}$  are  $\chi_{baa}^c$  and  $\chi_{aaa}^m$ . Then, the SH intensity  $I(2\omega)$  is proportional to  $|\chi_{baa}^c|^2$  for the  $p$ -polarized SH component ( $S_{in}\text{-}P_{out}$  configuration) and  $|\chi_{aaa}^m|^2$  for the  $s$ -polarized one ( $S_{in}\text{-}S_{out}$  configuration), respectively. The crystallographic component  $\chi_{baa}^c$  is arising from the presence of  $P$  along the  $b$  axis. On the other hand, the magnetic component  $\chi_{aaa}^m$  originates from  $T$  along the  $a$  axis.<sup>11</sup> Thus, the polarization-dependent measurements allow us to separate the crystallographic and magnetic SH components. Since the SH fields directly couple to  $P$  and  $T$ , we can detect the ultrafast  $P$  and  $T$  dynamics by all-optical method using the so-called pump-probe technique. Although the dynamics of  $M$  cannot be directly measured in the present case, it will be derived by comparing the dynamics of  $P$  and  $T$ , as discussed below.

An untwinned single crystal of GaFeO<sub>3</sub> was grown by a floating-zone method.<sup>5</sup> The  $ac$  surface of the crystal was polished for the optical measurements. For the femtosecond pump-probe spectroscopy, a Ti:sapphire regenerative amplifier system with the wavelength of 800 nm (1.55 eV), the pulse width of 130 fs, and the repetition rate of 1 kHz was used as the light source. The schematic illustration of the experiment is shown in the inset of Fig. 2(b). The  $s$ -polarized ( $E^\omega \parallel a$ ) incident probe light (frequency of  $\omega$ ), which was generated by using an optical parametric amplifier, was irradiated on the  $ac$  surface of the crystal. The generated  $s$ -polarized and  $p$ -polarized SH probe lights ( $2\omega$ ) were separated by a Rochon prism, isolated from the incident probe light by optical filters and monochromators, and detected by photomultiplier tubes. To obtain maximal intensities of the SH probe light, the photon energy of the incident probe light was set at 1.83 eV. In this case, the energy of the SH probe light (3.66 eV) is resonant with the peak energy of the charge-transfer (CT) transition band with a strong oscillator strength.<sup>11</sup> An external magnetic field of 1000 Oe, being enough to saturate the  $M$ , was applied along the  $c$  axis, namely, in the Voigt configuration. We have also measured the transient reflectivity change  $\Delta R/R$  at the photon energies  $\omega$  and  $2\omega$ . These signals were detected by a photodiode and used as a complementary probe of charge dynamics. Throughout all the measurements, the  $s$ -polarized pump lights were used.

Figure 1(b) shows the absorption coefficient  $\alpha$  spectra of GaFeO<sub>3</sub> at room temperature evaluated from the Kramers-Kronig transformation of the polarized reflectivity spectra.

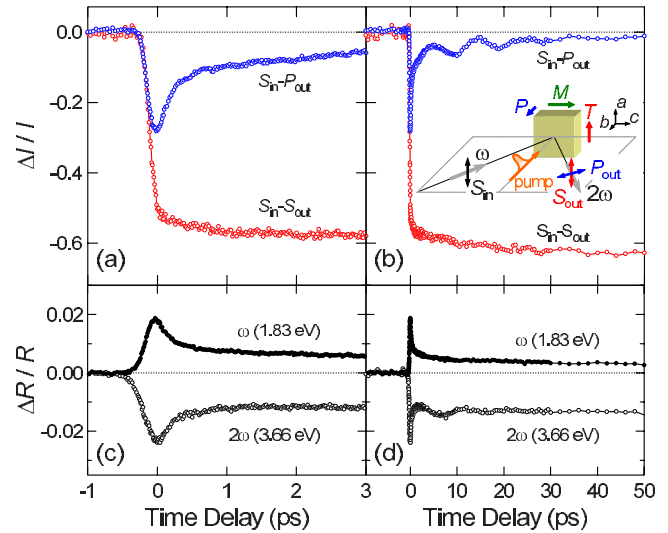


FIG. 2. (Color online) Time evolutions of (a), (b)  $\Delta I/I$  in the  $S_{in}\text{-}S_{out}$  and  $S_{in}\text{-}P_{out}$  configurations and (c), and (d)  $\Delta R/R$  in the  $S_{in}\text{-}S_{out}$  configuration at 1.83 and 3.66 eV at 50 K. The excitation density is 2.04 mJ/cm<sup>2</sup> in common. The schematic of time-resolved SHG is shown in the inset of (b).

The higher-lying ( $>3$  eV) intense absorption bands correspond to the CT excitations from the O  $2p$  to the Fe  $3d$  states.<sup>11,12</sup> Figure 1(c) shows the MSHG spectrum at 10 K in the  $S_{in}\text{-}S_{out}$  configuration on the  $ac$  surface [the inset of Fig. 1(c)] as a function of the SH photon energy.<sup>11</sup> Three peaks are observed around 2.84, 3.28, and 3.67 eV. These are assigned to the two-photon resonant transitions between the multiplets of Fe<sup>3+</sup> split by the crystal field, which are enhanced by the hybridization with the CT transition.<sup>11</sup>

First, we show in Figs. 2(a) and 2(b) the typical results for the time evolutions of the photoinduced changes in the SH intensities  $\Delta I/I$  in the  $S_{in}\text{-}S_{out}$  and  $S_{in}\text{-}P_{out}$  configurations at 50 K on the ultrafast ( $\sim 3$  ps) and the longer ( $\sim 50$  ps) time scales, respectively. The excitation density of the pump pulse is 2.04 mJ/cm<sup>2</sup>. Immediately after the photoexcitation, the rapid decrease in the SH intensities are observed in both the configurations, but their subsequent behaviors are considerably different from each other. These time profiles will reflect the dynamics of  $P$  and  $T$ , as described above. In deriving the dynamics of these two order parameters, we should consider that the SHG can be modified by the changes not only of  $\chi^c$  and  $\chi^m$  but also of the linear optical responses at  $\omega$  and  $2\omega$ , as given by the effective Fresnel factors.<sup>16-19</sup> To evaluate the latter effects, we measured the time evolutions of the reflectivity change  $\Delta R/R$  at the photon energies of the fundamental (1.83 eV) and the SH (3.66 eV) lights, the results of which are shown in Figs. 2(c) and 2(d), respectively. The excitation density is the same as that in the  $\Delta I/I$  measurements. The time profile at 3.66 eV is similar to that at 1.83 eV, although their signs are opposite. At 1.83 eV (3.66 eV) the excitation by the pump pulse leads to an increase (decrease) in reflectivity by  $\sim 2\%$ . This value is 1 order of magnitude smaller than those of  $\Delta I/I$ . This demonstrates that the change in the SH intensities is caused not by the modulation of the linear optical constants but by the direct modulation of  $P$  and  $T$ .

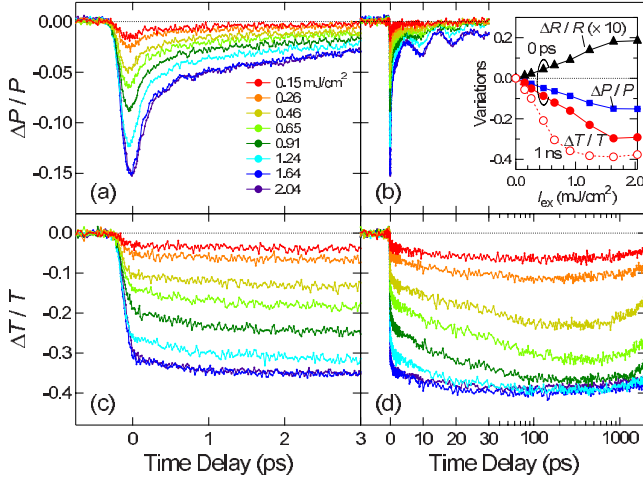


FIG. 3. (Color online) Time evolutions of (a), (b)  $\Delta P/P$  and (c), and (d)  $\Delta T/T$  at 50 K for different excitation densities. In the inset of (b), the excitation density dependence of  $\Delta P/P$ ,  $\Delta T/T$ , and  $\Delta R/R$  at 0 ps and  $\Delta T/T$  at 1 ns are shown.

On these bases, we can derive the changes of  $P$  and  $T$  from  $\Delta I/I$  in the  $S_{in}\text{-}P_{out}$  and  $S_{in}\text{-}S_{out}$  configurations by the following relations:

$$\Delta P/P = \sqrt{(\Delta I/I)_{SP} + 1} - 1, \quad (2)$$

$$\Delta T/T = \sqrt{(\Delta I/I)_{SS} + 1} - 1. \quad (3)$$

The obtained time evolutions of  $\Delta P/P$  and  $\Delta T/T$  at 50 K are shown in Figs. 3(a)–3(d) for different excitation densities. The  $P$  decreases immediately after the photoirradiation and then partly recovers within 1 ps: the residual part recovers with a few tens of picoseconds. The  $T$  also decreases upon the photoirradiation with possibly two components: the fast component appearing within 0.1 ps and the slow one with the rise time of  $\sim 10\text{--}30$  ps. The rise time of the fast component is nearly equal to that of  $P$ . The slow component almost saturates up to  $\sim 100$  ps and recovers to the initial state with the time scale of nanoseconds by the thermal diffusion. In addition, the oscillatory components with the period of  $\sim 10$  ps can be clearly seen in the time profile of  $\Delta P/P$  [and also  $\Delta I/I$  in the  $S_{in}\text{-}P_{out}$  configuration in Fig. 2(b) and  $\Delta R/R$  at 3.66 eV in Fig. 2(d)]. The spin precession is not the origin of the oscillation because its amplitude and period show negligible changes between 10 and 250 K. Typical frequencies of optical phonons are at least by 1 order of magnitude larger than that of the oscillation. From the results, it is natural to consider that this oscillation is not related to the spin dynamics but attributed to an acoustic shock wave transmitting from the surface into inside bulk.<sup>20</sup> In the inset of Fig. 3(b), we plot the excitation density dependence of  $\Delta P/P$ ,  $\Delta T/T$ , and  $\Delta R/R$  at 0 ps (Ref. 21) and  $\Delta T/T$  at 1 ns. Interestingly, the three quantities at 0 ps show quite similar behaviors, likely indicating that the initial decreases of  $P$  and  $T$  are governed by the identical origin, that is, the generation of the CT excited states or the photocarrier generations. On the other hand,  $\Delta T/T$  at 1 ns shows different excitation density dependence.

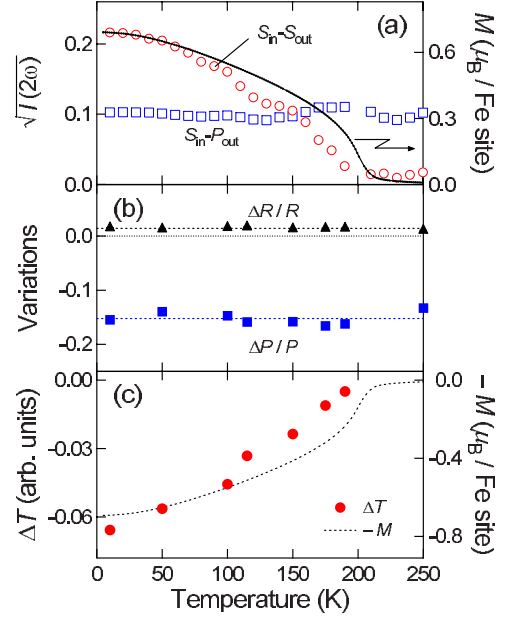


FIG. 4. (Color online) (a) Temperature dependence of the square root of the static SH intensity  $\sqrt{I(2\omega)}$  in the  $S_{in}\text{-}P_{out}$  and  $S_{in}\text{-}S_{out}$  configurations. A solid line represents the magnetization measured in a field-cooling run under a magnetic field of 1000 Oe applied along the  $c$  axis. (b) Temperature dependence of  $\Delta P/P$  and  $\Delta R/R$  at 0 ps with excitation density of  $1.85$  mJ/cm<sup>2</sup>. (c) Temperature dependence of  $\Delta T$  at 0 ps. The magnetization curve inverted in sign is also shown by the dotted line for comparison.

Next, we show the results of the temperature dependence. Figure 4(a) shows the square root of the static SH intensities  $\sqrt{I(2\omega)}$  in the  $S_{in}\text{-}P_{out}$  and  $S_{in}\text{-}S_{out}$  configurations as a function of temperature. It was confirmed that the SH intensities in both the configurations did not depend on the direction of the magnetic field. As mentioned above,  $\sqrt{I(2\omega)}$  is proportional to  $|\chi_{baa}^c|$  for the  $S_{in}\text{-}P_{out}$  configuration and  $|\chi_{aaa}^m|$  for the  $S_{in}\text{-}S_{out}$  configuration, respectively. The results indicate that  $|\chi_{baa}^c|$  does not change with temperature. This is consistent with the crystalline-lattice nature of  $P$  in GaFeO<sub>3</sub>.<sup>10,11</sup> As a result, the temperature dependence of  $|\chi_{aaa}^m|$ , which is determined by the temperature dependence of  $T$ , coincides with that of  $M$  presented by a solid line in Fig. 4(a). In Fig. 4(b) the temperature dependences of  $\Delta P/P$  and  $\Delta R/R$  at 0 ps are shown with excitation density of  $1.85$  mJ/cm<sup>2</sup>.  $\Delta P/P$  shows little temperature variation as well as  $\Delta R/R$ . On the other hand,  $|\Delta T|$  at 0 ps shown in Fig. 4(c) becomes smaller as the temperature is increased from 10 K and finally disappears around  $T_C$ .

On the basis of these results, we discuss the ultrafast dynamics of the multiferroic properties, i.e.,  $P$ ,  $M$ , and  $T$ . Of these, the dynamics of  $M$  is derived by comparing the  $P$  and  $T$  dynamics because  $\Delta M$  cannot be extracted from the simple arithmetic of  $\Delta P$  and  $\Delta T [\propto \sum_i (\Delta r_i \times s_i + r_i \times \Delta s_i)]$  in the present case. First, the time evolution of  $P$ , in both rise and decay processes, quite resembles that of  $R$ , as is obvious from Figs. 2 and 3. Considering that the time evolution of  $R$  reflects the photocarrier dynamics, the CT excitation and the resultant carrier generation appear to instantaneously disrupt the spontaneous  $P$  through the changes in the charge distri-



bution and/or the atomic displacements ( $r_i$ ). Then, the recovery of  $P$  occurs with no delay after the relaxation of the CT excited states. On the other hand, the time evolution of  $T$  shows a different behavior, consisting of the fast and slow components, as mentioned above. It is natural to consider that such a difference between  $P$  and  $T$  dynamics is caused by the dynamics of  $M$ . Up until now, the photoinduced demagnetization dynamics has been extensively studied in ferromagnetic or ferrimagnetic materials.<sup>22–25</sup> In most cases, the main decrease of  $M$  is caused by the thermalization of the spin system through the spin-lattice interaction. In addition, the relatively fast demagnetization is sometimes observed, which has been attributed to the emissions of magnetic excitations during nonradiative decay of photocarriers.<sup>25</sup> Its rise time is, therefore, almost equal to the decay time of photocarriers. For the former thermalization process, the systematic studies by means of the time-resolved magneto-optical Kerr effect revealed that the time constant  $\tau$  for the spin thermalization is proportional to the inverse of the magneto-crystalline anisotropy usually expressed by  $K$ .<sup>25</sup> Using this scaling law and the  $K$  value of  $(1–5) \times 10^5$  J/m<sup>3</sup> at 50 K for GaFeO<sub>3</sub>,<sup>26,27</sup>  $\tau$  can be estimated as 5–50 ps. The observed time constant (10–30 ps) for the slow component in the dynamics of  $T$  is consistent with this estimated value. This result suggests that the slow decrease of  $T$  is attributable to the decrease of  $M$  due to the thermalization of the spin system.

On the other hand, the fast decrease of  $T$  within 0.1 ps is even faster than the decay of photocarriers ( $\sim 0.3$  ps) esti-

mated from Fig. 2(c). This suggests that the emissions of magnetic excitations are not relevant to this process. For such an ultrafast response of  $T$ , the contribution from the simple  $P$  modulation will be basically large, as deduced from the similarity in the initial  $P$  and  $T$  dynamics. In this case because  $\Delta P (= \sum_i \Delta r_i)$  hardly depends on temperature, as shown in Fig. 4(b), the temperature dependence of  $\Delta T$  (from  $\sum_i \Delta r_i \times s_i$  term) will be similar to that of  $M (= \sum_i s_i)$ , as is in fact seen in Fig. 4(c). In addition, taking into account the fact that the linear ME effect in GaFeO<sub>3</sub> is dominated by  $T$ ,<sup>4,5</sup> a bilinear coupling between  $P$  and  $M$ , which leads to the occurrence of  $\Delta s_i^{me}$  when  $r_i$  changes, may be also important in such a multiferroic as GaFeO<sub>3</sub>. Although  $\Delta s_i^{me}$  should contribute to  $\Delta T$ , it is difficult to extract such a ME component out of the total  $\Delta T$  due to the large contribution from the simple  $P$  modulation. However, the understanding of the ME response on various time scales is of paramount importance for the development of practical devices with the ME functionality. As we have demonstrated here, the time-resolved nonlinear optical techniques will offer a great advantage in investigating the dynamical behaviors of multiple degrees of freedom and their interaction in multiferroics. Moreover, in line with the future progress of such studies, the ME mechanism may provide a unique route to effectively control the magnetic state on an ultrafast time scale.

We would like to thank Y. Ogawa who supplied the MSHG spectrum of GaFeO<sub>3</sub>.

- <sup>1</sup>T. Kimura, T. Goto, H. Shintani, K. Ishizaka, T. Arima, and Y. Tokura, *Nature* (London) **426**, 55 (2003).
- <sup>2</sup>N. A. Spaldin and M. Fiebig, *Science* **309**, 391 (2005).
- <sup>3</sup>M. Fiebig, *J. Phys. D* **38**, R123 (2005).
- <sup>4</sup>Yu. F. Popov, A. M. Kadomtseva, G. P. Vorob'ev, V. A. Timofeeva, D. M. Ustinin, A. K. Zvezdin, and M. M. Tegeranchi, *J. Exp. Theor. Phys.* **87**, 146 (1998).
- <sup>5</sup>T. Arima, D. Higashiyama, Y. Kaneko, J. P. He, T. Goto, S. Miyasaka, T. Kimura, K. Oikawa, T. Kamiyama, R. Kumai, and Y. Tokura, *Phys. Rev. B* **70**, 064426 (2004).
- <sup>6</sup>B. B. Van Aken, J.-P. Rivera, H. Schmid, and M. Fiebig, *Nature* (London) **449**, 702 (2007).
- <sup>7</sup>H. Schmid, *Ferroelectrics* **252**, 253 (2001).
- <sup>8</sup>J. H. Jung, M. Matsubara, T. Arima, J. P. He, Y. Kaneko, and Y. Tokura, *Phys. Rev. Lett.* **93**, 037403 (2004).
- <sup>9</sup>M. Kubota, T. Arima, Y. Kaneko, J. P. He, X. Z. Yu, and Y. Tokura, *Phys. Rev. Lett.* **92**, 137401 (2004).
- <sup>10</sup>T. Arima, J. H. Jung, M. Matsubara, M. Kubota, J. P. He, Y. Kaneko, and Y. Tokura, *J. Phys. Soc. Jpn.* **74**, 1419 (2005).
- <sup>11</sup>Y. Ogawa, Y. Kaneko, J. P. He, X. Z. Yu, T. Arima, and Y. Tokura, *Phys. Rev. Lett.* **92**, 047401 (2004).
- <sup>12</sup>A. M. Kalashnikova, R. V. Pisarev, L. N. Bezmaternykh, V. L. Temerov, A. Kirilyuk, and Th. Rasing, *JETP Lett.* **81**, 452 (2005).
- <sup>13</sup>*Nonlinear Optics in Metals*, edited by K. H. Bennemann (Clarendon, Oxford, 1998).
- <sup>14</sup>M. Fiebig, D. Fröhlich, B. B. Krichevstov, and R. V. Pisarev, *Phys. Rev. Lett.* **73**, 2127 (1994).
- <sup>15</sup>M. Fiebig, Th. Lottermoser, D. Fröhlich, A. V. Goltsev, and R. V. Pisarev, *Nature* (London) **419**, 818 (2002).
- <sup>16</sup>J. Hohlfeld, U. Conrad, and E. Matthias, *Appl. Phys. B: Lasers Opt.* **63**, 541 (1996).
- <sup>17</sup>A. Melnikov, I. Radu, U. Bovensiepen, O. Krupin, K. Starke, E. Matthias, and M. Wolf, *Phys. Rev. Lett.* **91**, 227403 (2003).
- <sup>18</sup>N. P. Duong, T. Satoh, and M. Fiebig, *Phys. Rev. Lett.* **93**, 117402 (2004).
- <sup>19</sup>T. Satoh, B. B. Van Aken, N. P. Duong, T. Lottermoser, and M. Fiebig, *Phys. Rev. B* **75**, 155406 (2007).
- <sup>20</sup>From the oscillation period and the refractive index for the probe light, the sound velocity is evaluated to be  $\sim 7.7$  km/s, which is close to the value reported in other oxides, see M. Fiebig, K. Miyano, Y. Tomioka, and Y. Tokura, *Appl. Phys. B: Lasers Opt.* **71**, 211 (2000).
- <sup>21</sup>Here, 0 ps means the time when  $\Delta P/P$  (or  $\Delta R/R$ ) shows minimum around the time origin.
- <sup>22</sup>E. Beaurepaire, J.-C. Merle, A. Daunois, and J.-Y. Bigot, *Phys. Rev. Lett.* **76**, 4250 (1996).
- <sup>23</sup>J. Hohlfeld, E. Matthias, R. Knorren, and K. H. Bennemann, *Phys. Rev. Lett.* **78**, 4861 (1997).
- <sup>24</sup>B. Koopmans, M. van Kampen, J. T. Kohlhepp, and W. J. M. de Jonge, *Phys. Rev. Lett.* **85**, 844 (2000).
- <sup>25</sup>T. Ogasawara, K. Ohgushi, Y. Tomioka, K. S. Takahashi, H. Okamoto, M. Kawasaki, and Y. Tokura, *Phys. Rev. Lett.* **94**, 087202 (2005).
- <sup>26</sup>A. Pinto, *J. Appl. Phys.* **37**, 4372 (1966).
- <sup>27</sup>B. F. Levine, C. H. Nowlin, and R. V. Jones, *Phys. Rev.* **174**, 571 (1968).